Journal Pre-proof

The impact of water on Firefighter protective clothing thermal performance and steam burn occurrence in firefighters

André Fonseca Malaquias, S.F. Neves, J.B.L. M. Campos

PII: S0379-7112(21)00248-4

DOI: https://doi.org/10.1016/j.firesaf.2021.103506

Reference: FISJ 103506

To appear in: *Fire Safety Journal*

Received Date: 20 July 2021

Revised Date: 26 November 2021

Accepted Date: 28 November 2021

Please cite this article as: André.Fonseca. Malaquias, S.F. Neves, J.B.L. M. Campos, The impact of water on Firefighter protective clothing thermal performance and steam burn occurrence in firefighters, *Fire Safety Journal* (2022), doi: https://doi.org/10.1016/j.firesaf.2021.103506.

The Impact of Water on Firefighter Protective Clothing Thermal Performance and Steam Burn Occurrence in Firefighters

André Fonseca Malaquias*, S. F. Neves, J.B.L.M. Campos

CEFT, Transport Phenomena Research Centre, Engineering Faculty of Porto University, Porto, Portugal

Abstract

Exposure to oscillating heat fluxes while having variable water contents in the thermal protective clothing (T.P.C) is possible in a real firefighting scenario. The occurrence of steam burns becomes inevitable in certain conditions which are still unidentified in the literature. In light of such, in this study, the effect of water distribution on thermal protective clothing (T.P.C) performance is studied for various environmental conditions (i.e., fixed and transient values of heat flux). A numerical approach is used to simulate heat and mass transport in the T.P.C.. Parametric studies are performed, where the exposure heat flux (0 - 80 kW/m^2) and initial quantities of water in the T.P.C. are varied and correlated with second–degree burn times. The presence of water in the outer shell increases second-degree burn times, while water in the inner layer has the opposite effect for high heat fluxes. For the tested heat fluxes, burns obtained are majorly of a scald nature. The results generated allow for identifying environmental and protective clothing conditions where steam burns may become a potential hazard. This study can directly impact the proceedings for firefighters to take in certain environmental conditions and aid in the design of more effective firefighting protective suits.

Keywords: Firefighting garment; Water transport; Numerical simulation; Steam burns; second-degree burns; initial water content.

*Corresponding author: E-mail: up201007676@up.pt (A. Fonseca Malaquias)

1. Introduction

Firefighters face high heat flux and humid scenarios, exposing them to potential heat stress illness and skin burns [1–3]. During fire combat, firefighters may suffer burns caused by direct heat from the flame and high-temperature vapor reaching the skin and condensing [4,5].

High humid environments in firefighting make the task of designing adequate firefighting clothing challenging. The presence of water in firefighting garments is frequent, either due to firefighters sweating during strenuous exercise or due to external sources [3,6,7]. Water presence in a firefighting garment assembly significantly alters its thermal performance. However, the current evaluation norms do not consider transient moisture effects when measuring firefighting clothing performance [8].

In the meantime, various researchers have, mostly experimentally, studied the influence of moisture in firefighting clothing performance.

Su et al. [5] studied the effects of different initial moisture contents in firefighting clothing thermal performance. Two thermal inners with different weights were initially incorporated with various amounts of water (0 – 100 % wt. of turnout system), simulating the presence of sweat in the firefighting jacket. Afterward, the layers were exposed to a radiative heat flux of 8.5 kW/m^2. The authors increased the initial water content and a convex trend was noticed for second-degree burn time (i.e., a minimum occurs at 50 % wt. of turnout system). A similar conclusion was reached, for third-degree burn time, with the minimum verified at 15 % wt.

He et al. [9] used a modified thermal protective performance (T.P.P.) test apparatus to study the exposure of pre-moistened firefighting jackets (0-70 % wt. of turnout system) to a radiative heat flux of 21 kW/m^2. The authors also studied the influence of air gap size and location. Second-degree burn time decreased with an increase in moisture content for most air gap configurations. A minimum trend with water content was also observed, at 20 % wt. of moisture content for most cases. Barker et al. [10] also experimentally studied the effect of different moisture contents initially present (0-100 % wt. of turnout system) in the thermal inner, on the second-degree burn time, for a heat flux of 6.3 kW/m^2. However, contrary to the previously mentioned studies, more complicated moisture effects were observed; a maximum burn time for 50 % wt. moisture incorporation, superior to that of the dry textile (i.e., 0 % wt.).

Lawson et al. [7] utilized four different two-layered firefighting jackets to study the influence of moisture. The outer shell and thermal inners were either assumed to be dry, conditioned at specific atmospheric conditions, or in their saturated state. The fabric system was exposed to low–radiant flux (10 kW/m^2) or high-radiant flux (83 kW/m^2). The authors showed that water in the outer layer was beneficial for high heat fluxes but prejudicial in the inner layer. For low heat fluxes, however, water in the thermal inner was advantageous towards thermal performance. They also highlighted the dependence of the results on the textile materials used in the experiments.

Keiser & Rossi [11] incorporated moisture in the thermal barrier (278 % - 696 % wt. of thermal barrier) or underwear (70 % - 176 % wt. of underwear), and exposed a 5–layered firefighting jacket to a radiative flux of 5 kW/m^2 for 10 min. The authors concluded that the presence of moisture decreases the temperatures in the garment. The same group performed a study using X-ray radiography [4] and validated the temperature sensor-based approach to measure, indirectly, the humidity concentrations in the previous study. They confirmed that the moisture initially present in outer layers might re-condense near the skin, originating steam burns.

Onofrei et al. [12] also studied the effect of moisture presence on thermal performance for low–heat fluxes. They incorporated the moisture in the thermal inner (120 % to 200 % wt. of thermal inner) of a 3 or 4 layer firefighting jacket exposed to a low radiant heat flux of 1.1 kW/m^2. They found that the presence of moisture decreases temperatures in the protective clothing over the exposure time. Zhang et al. [6] studied the effect of the moisture in the outer shell and in the thermal inner of a 3-layered firefighting garment when exposed to a heat flux of 15.4 kW/m^2. The authors noticed an increase in second-degree burn time with outer shell moisture but a diminishment when moisture was also present in the thermal inner.

From the studies above, precise conclusions about the influence of moisture on thermal performance under diverse heat exposures are hard to obtain. This difficulty is due to several issues, including different material properties, experimental conditions, and set-ups. Also, contradictory results between some works exist, and the reasons why are not well understood.

In parallel, several authors have developed numerical models to understand better heat and mass transfer mechanisms in firefighting garments. Chitrphiromsri [13] incorporated a heat and moisture transfer model to study heat transfer in a flash fire scenario (84 kW/m^2 for 4 s) with the presence of liquid water in a typical 3– layered firefighting jacket. The authors assumed an initial moisture content present in all 3 –layers corresponding to 10 % of the saturation point of each respective layer.

Prasad et al. [3] proposed a heat and moisture transfer model for a firefighting jacket and validated it for an exposure of 2.5 kW/m^2 for 750 s, assuming an initially wet thermal inner. The authors showed a thermal performance enhancement with moisture incorporation in the thermal inner compared to dry textiles. Su et al. [14] numerically studied the heat and moisture transport in a 3 –layer firefighting jacket exposed to a low heat flux (8.5 kW/m^2 for 300 s followed by a 200 s cooling period). The authors concluded that while moisture decreases the heat flux towards the skin, it increases thermal hazard due to higher stored energy in the garment. Huang et al. [15]

numerically studied the relative humidity (0-90 % R.H) effect on the thermal performance of a 3 – layer protective firefighting jacket exposure to a flux of 5 kW/m^2. They found a positive trend between relative humidity and second–degree burn time. Łapka et al. [16] outlined a heat and moisture transport model for a three-layer firefighting protective clothing fabric. The model accounted for fabric movement and its influence on heat and water vapor transport in the garment.

In resume, in the literature, most studies in the area are experimental. It is hard to achieve coherent conclusions in these studies as different experimental set-ups and garments, measuring techniques, and protocols are utilized. No systematic study has been conducted considering a wide range of heat flux scenarios, nor real exposure scenarios. Hence any comparison, and trends, between the studies are not conclusive. Also, current numerical models in the literature lack details regarding the condensation phenomena in the textile when mass fluxes are significant. No results have been shown or discussed for cases when the different garment layers contain different saturation levels of free water. This aspect is essential to consider, as it can happen in real firefighting scenarios.

Hence, in light of such, an extensive and systematic numerical study was carried out. Firstly, the apart effects of the initial moisture content in the outer shell and thermal inner were studied for a wide variety of heat fluxes. Then, both layers were assumed to have different initial water quantities simultaneously. The effect of such water distribution in the thermal performance was analyzed for various heat flux exposures. Lastly, to apply the concepts, a live-fire training exercise consisting of a highly transient heat flux exposure was considered, and the respective effects on temperature and water profiles were discussed.

2. Materials and Methods

2.1 Problem description

A typical 3-layered firefighting protective clothing (F.F.P.C) was assumed (Figure 1). Also, a 3 – layered skin model was used to simulate the firefighter's presence in contact with the F.F.P.C.

Initially, a firefighter wearing the F.F.P.C. is exposed to an external thermal hazard (boundary 1, Figure 1). Consequently, the temperature in the layers of the garment starts rising. Liquid water initially present in the garment due to sweat or ambient exposure starts evaporating and diffusing, reducing the temperature rate increase. Some of this vapor may be rejected towards the ambient (i.e., evaporative cooling) or diffuse and re-condense near the skin, liberating condensation heat. After some exposure time, the firefighter may suffer skin burns due to the direct heat from the thermal hazard or moisture re-condensation near the skin or a combination of both.

Core body temperature was assumed constant at 37 ºC (boundary 2, Figure 1) throughout the exposure. Firefighters may have a higher core temperature when entering a fire scenario (e.g., 38 ºC); however, such is unlikely to influence second-degree burn times due to the thermal resistance between the core and the epidermis (2*). Fabrics' properties are shown with their respective sources in Table 1. Some of the properties missing had to be estimated to perform numerical simulations.

Figure 1- F.F.P.C. skin system used in the numerical simulations with the indication of the boundary numbers.

The moisture distribution effect on the thermal protective performance was studied, assuming a uniform initial moisture distribution in each fabric layer. Similar water distribution was taken by Chitrphiromsri [13]. The initial temperature at the skin layers was assumed to have a linear profile between the core temperature (37 ºC) and skin temperature (34 ºC). The garment's initial temperature and relative humidity were assumed to be 34 ºC and 65 %, respectively.

Table 1 – Properties of the various layers consisting of the firefighting protective clothing.

Property	Outer shell	Moisture Barrier	Thermal inner	Source
Thickness (w) mm	0.39	0.45	2.24	[6]
Density (ρ_{ds}) kg/m^3	1460	1460	1440	[6]
Specific heat (c_{ds}) J/(kg K)	1086	1086	1421	[17]
Thermal conductivity (k_{ds}) W/(m K)	0.25	0.25	0.21	[17,18]
Fiber volume fraction (ε_{ds})	0.36	0.16	0.09	Estimated [6,19]
Tortuosity (τ)	2.32	2.87	1.32	Estimated [12]
Fiber diameter (d_f) µm	15	15	15	[6,20]
Regain at 65 % RH	0.0485	0.0485	0.0397	[14]
Diffusivity of water in fiber (D_f) m^2/s	6×10^{-14}	6×10^{-14}	6×10^{-14}	[13]
Proportionality constant for liquid water sorption in fibres (γ_{ls}) kg/m^3	5×10^{-4}	5×10^{-4}	5×10^{-4}	[13]

2.2 Mathematical model and assumptions

2.2.1 **Textile model**

A model similar to the one suggested by Chitrphiromsri [13], based on Gibson's model [21], was assumed to perform the one-dimensional numerical analysis. The most important assumption is that homogeneous phases can well describe the heterogeneous porous hygroscopic structure of the textile layer with different materials (i.e., gas, solid, liquid) [21]. Heat and moisture transport occur throughout and between the phases where moisture may transfer (e.g., water from gas to liquid phase). Using Gibson's model, problems associated with geometric domain definition are eliminated, promoting computer efficiency.

The model in the textile layers comprises one global energy balance and three species transport balances (i.e., water transport in the gas, fiber, and liquid phase). Fourier type heat transfer is assumed to simulate the heat transport in the firefighting garment. Hence for a hygroscopic medium, where water sorption and condensation may take place, and assuming heat conduction to be the effective heat transfer mechanism, the global energy balance is written as follows:

$$\rho_{eff}C_{eff}\frac{\partial T}{\partial t}+\frac{\partial}{\partial x}\left(-k_{eff}\frac{\partial T}{\partial x}\right)-\dot{m}_{gs}\left(\Delta h_{vap}+\Delta h_l\right)-\dot{m}_{gl}\Delta h_{vap}-\dot{m}_{ls}\Delta h_l=0 \qquad \text{eq. 1a}$$

$$\rho_{eff}=\varepsilon_{bw}\rho_w+\varepsilon_\gamma\rho_\gamma+\varepsilon_{ds}\rho_{ds}+\varepsilon_l\rho_w \qquad \text{eq. 1b}$$

$$C_{p,eff}=\frac{\varepsilon_{bw}\rho_w c_{p,w}+\varepsilon_\gamma\left(\rho_a c_{p,a}+\rho_v c_{p,v}\right)+\varepsilon_{ds}\rho_{ds}c_{p,ds}+\varepsilon_l\rho_w c_{p,w}}{\rho_{eff}} \qquad \text{eq. 1c}$$

$$k_{eff}=k_\gamma\left\{\frac{\varepsilon_\gamma k_\gamma+[1+\varepsilon_{bw}+\varepsilon_{ds}+\varepsilon_l]k_\sigma}{\varepsilon_\gamma k_\sigma+[1+\varepsilon_{bw}+\varepsilon_{ds}+\varepsilon_l]k_\gamma}\right\} \qquad \text{eq. 1d}$$

where, ρ_{eff}, C_{eff}, k_{eff}, $\dot{m}_{gs}$, $\dot{m}_{gl}$, $\dot{m}_{ls}$, Δh_{vap} and Δh_l represent the effective density (kg/m^3), effective specific heat (J/(kg K)), effective thermal conductivity (W/(m K)), gas sorption/desorption rate (kg/(m^3 s)), vaporization/condensation rate (kg/(m^3 s)), liquid sorption/desorption rate (kg/(m^3 s)), water vaporization heat (J/kg), and liquid sorption/desorption heat (J/kg), respectively. ε represents the phase volume fraction, and the subscripts *bw*, *w*, *γ*, *ds*, and *l* stand for bounded water, water, gas, fiber, and liquid, respectively.

The first term on the left-hand side of eq.1a accounts for the heat accumulation in the garment. The second term accounts for the conductive heat fluxes, while the third, fourth and fifth terms account for the latent heat associated with water sorption/desorption, vaporization/condensation and liquid sorption/desorption into the fibers, respectively. k_σ and k_γ represent the solid and gas phases thermal conductivity respectively, and they are calculated as follows:

$$k_\sigma = \frac{k_w \rho_w \varepsilon_{bw} + k_{ds} \rho_{ds} \varepsilon_{ds} + k_w \rho_w \varepsilon_l}{\rho_w \varepsilon_{bw} + \rho_{ds} \varepsilon_{ds} + \rho_w \varepsilon_l} \quad \text{eq. 1e}$$

$$k_\gamma = \frac{k_v \rho_v + k_a \rho_a}{\rho_v + \rho_a} \quad \text{eq. 1f}$$

where subscripts v, a, refer to the water vapor and air, respectively.

Water vapor transport in the gas phase is calculated as follows:

$$\frac{\partial(\varepsilon_\gamma \cdot \rho_v)}{\partial t} + \frac{\partial}{\partial x}\left(-D_{eff} \frac{\partial \rho_v}{\partial x}\right) + \dot{m}_{gs} + \dot{m}_{gl} = 0 \quad \text{eq. 2a}$$

$$D_{eff} = \frac{\varepsilon_\gamma \cdot D_a}{\tau} \quad \text{eq. 2b}$$

$$D_a = 2.23 \cdot 10^{-5} \left(\frac{T}{273.15}\right)^{1.75} \quad \text{eq. 2c}$$

where ρ_v, D_{eff}, D_a, and τ stand for water vapor density (kg/m^3), effective diffusivity throughout the textile layer (m^2/s), water vapor diffusivity in the air (m^2/s), and fabric tortuosity, respectively.

The first term of eq.2a refers to vapor accumulation in the gas phase, the second term accounts for diffusive water vapor transport, and the third and fourth terms account for sorption/desorption and condensation/evaporation of water, respectively.

The liquid water and bounded water transport balances are as follows:

$$\rho_w \frac{\partial \varepsilon_l}{\partial t} = \dot{m}_{sl} + \dot{m}_{vl} \quad \text{eq. 3}$$

$$\rho_w \frac{\partial \varepsilon_{bw}}{\partial t} = \dot{m}_{gs} + \dot{m}_{ls} \quad \text{eq. 4}$$

As can be seen, there is no convective or diffusive transport of liquid and bounded water. Only terms associated with water phase changes are considered. They are calculated as follows:

$$\dot{m}_{gs} = \frac{8D_f \rho_{ds}}{d_f^2}\left(Regain_{eq} - Regain_f\right) \quad \text{eq. 5a}$$

where D_f, d_f, and *Regain* represent water diffusivity in the clothing fiber (m^2/s), fiber diameter (m), and fabric regain, respectively.

$$\dot{m}_{gl} = \begin{cases} c \cdot \left(\rho_v - \rho_{v,sat}\right) \\ h_m a_s \frac{\varepsilon_l}{\varepsilon_l^{cr}}\left(\rho_v - \rho_{v,sat}\right) \end{cases} \quad \text{eq. 5b}$$

where *c* represents a correction factor (i.e., 10^5 s^{-1}) which accounts for the instantaneous condensation when the pores become saturated with water vapor. The variable ε_l^{cr} represents the critical liquid water fraction for which water movement starts occurring in the pores (defined as $\varepsilon_l^{cr} = s \cdot \varepsilon_g^{init}$ where *s* stands for the saturation level in which liquid water movement starts occurring in the textile). In this work, the saturation levels were defined as 0.77, 0.1, 0.27 for the outer, moisture, and thermal inner, respectively. The variables h_m and a_s represent the mass transfer coefficient between the fiber and the surrounding air (m/s), and the specific surface area (m^{-1}) is defined as:

$$a_s = \frac{4\varepsilon_{ds}}{d_f} \quad \text{eq. 5c}$$

$$\dot{m}_{ls} = h_m a_s \gamma_{ls} \frac{\varepsilon_l}{\varepsilon_l^{cr}}\left(\frac{Regain_{eq}}{Regain_f} - 1\right) \quad \text{eq. 5d}$$

where γ_{ls} is the sorption proportionality constant of liquid water in the fiber; the subscripts *eq* and *f* stand for equilibrium and fabric, respectively.

The fabric regain is calculated as follows:

$$Regain_f = \frac{\varepsilon_{bw}\rho_w}{\varepsilon_{ds}\rho_{ds}} \qquad \text{eq. 5e}$$

and the equilibrium regain by:

$$Regain_{eq} = \frac{\varepsilon_{bw}|_{eq} \cdot \rho_w}{\varepsilon_{ds}\rho_{ds}} = 0.578 \cdot Regain_{f(\emptyset=65\,\%)} \cdot \emptyset \cdot \left[(0.321+\emptyset)^{-1} + (1.262-\emptyset)^{-1}\right] \qquad \text{eq. 5f}$$

where Ø is the relative humidity.

Lastly, the volume fractions of each phase must satisfy the following constraint:

$$\varepsilon_{ds} + \varepsilon_{bw} + \varepsilon_{\gamma} + \varepsilon_{l} = 1 \qquad \text{eq.6}$$

Other thermodynamic relations regarding the model are below:

$$p_v = \frac{\rho_v RT}{M_{H_2O}} \qquad \text{eq. 7a}$$

$$\rho_\gamma = \rho_v + \rho_a \qquad \text{eq. 7b}$$

$$p_a = p_\gamma - p_v \qquad \text{eq. 7c}$$

where p_γ, p_v, R and M_{H_2O} stand for the total pressure (Pa), partial vapor pressure (Pa), universal gas constant (J/(mol K)) and water molecular mass (kg/mol), respectively.

2.2.2 Skin model

The Pennes' bio-heat model was assumed to describe the heat exchanges in the firefighter's skin layers. The following equations describe heat transport in the epidermis, dermis and subcutaneous:

$$\rho_{ep} C_{ep} \frac{\partial T}{\partial t} = \frac{\partial}{\partial x}\left(k_{ep}\frac{\partial T}{\partial x}\right) \qquad \text{eq. 8a}$$

$$\rho_{derm} C_{derm} \frac{\partial T}{\partial t} = \frac{\partial}{\partial x}\left(k_{derm} \frac{\partial T}{\partial x}\right) - G\rho_b c_b (T - T_c) \quad \text{eq. 8b}$$

$$\rho_{subcut} C_{subcut} \frac{\partial T}{\partial t} = \frac{\partial}{\partial x}\left(k_{subcut} \frac{\partial T}{\partial x}\right) - G\rho_b c_b (T - T_c) \quad \text{eq. 8c}$$

where G, ρ_b, c_b and T_c represent the volumetric blood flow, blood density (kg/m^3), specific heat (J/(kg K)) and core body temperature (K), respectively. The subscripts *ep*, *derm*, and *subcut* stand for epidermis, dermis and subcutaneous, respectively. The properties of the skin layers are in Table 2.

Like other studies in the field, Henriques' burn criterion was utilized to calculate second-degree burn time [22].

Table 2 - Properties of skin layers taken from [13].

Property	epidermis	dermis	Subcutaneous
Thermal conductivity (k) W/(mK)	0.255	0.523	0.167
Specific heat (c_p) J/(kg K)	3600	3400	3060
Density (ρ) kg/m^3	1200	1200	1000
Thickness (w) mm	0.08	2	10
Blood perfusion rate (G) s^{-1}	1.25×10^{-3}	1.25×10^{-3}	1.25×10^{-3}

2.3 Boundary and initial conditions

Donnelly et al. [23] divided the firefighting scenario into four thermal classes that a firefighter can face. These classes are categorized based on the heat flux and air temperature. In this work, an effort to consider heat flux exposures covering all types was made. Total heat fluxes in the range from 5-80 kW/m^2 were selected to simulate pre-flashover and flash fire conditions (Neumann condition imposed at boundary 1, Figure 1). A constant core body temperature of 37 ^{o}C (Dirichlet condition imposed at boundary 2, Figure 1) and ambient temperature of 34 ^{o}C with 65 % R.H. were considered throughout the simulation. A Newmann boundary condition in the outer shell for mass transfer between the garment and the environment was assumed (eq. 9a;

imposed at boundary 1, Figure 1), while a mass insulation condition at the boundary facing the skin (2*, Figure 1) was set:

$$k_c(\rho_v - \rho_{amb}) = -D_{eff,outer}\left.\frac{\partial \rho_v}{\partial x}\right|_{x=0} \qquad \text{eq. 9a}$$

where k_c represents the mass transfer coefficient (0.021 m/s) [13].

The initial conditions assumed are shown in Table 3.

Table 3 - Initial conditions assumed for the firefighting protective clothing

Property	Outer shell	Moisture Barrier	Thermal Inner
$\varepsilon_{l,init}$	Distribution (0 to 0.27) (i.e. wetness level 0 to 1)	0	Distribution (0 to 0.25) (i.e. wetness level 0 to 1)
$\varepsilon_{b,init}$	0.025	0.007	0.008
T_{init}	34 ºC	34 ºC	34 ºC
$Ø_{init}$	0.65	0.65	0.65

The initial temperature at the skin is assumed to be a linear gradient between 34 ºC at the epidermis surface and 37 ºC at the subcutaneous core. Note that the distributions mentioned for the initial water fractions correspond to wetness levels between 0 and 1 for the outer shell and thermal inner.

2.4 Grid independence tests

To ensure solution accuracy and promote computational efficiency, grid convergence tests concerning time and space were performed. Figure 2a shows the difference in skin temperature histories obtained with the different indicated meshes in Table 4. As can be seen, spatial mesh independence is obtained with Mesh 2. The same can be said regarding vapor densities, vaporization/condensation and sorption rates near the skin (Figure 2c, e and g). A backward differentiation formula solver was used to choose the best time step, utilizing a relative tolerance as a criterion. The best relative tolerance obtained was 10^{-4} and a residual-based termination criterion was used (Figure 2b, d, f and g).

Table 4 - Meshes used to test spatial mesh independence

Mesh no.	Elements in textile	Elements in skin
Mesh 1	50	5
Mesh 2	500	50
Mesh 3	1000	100

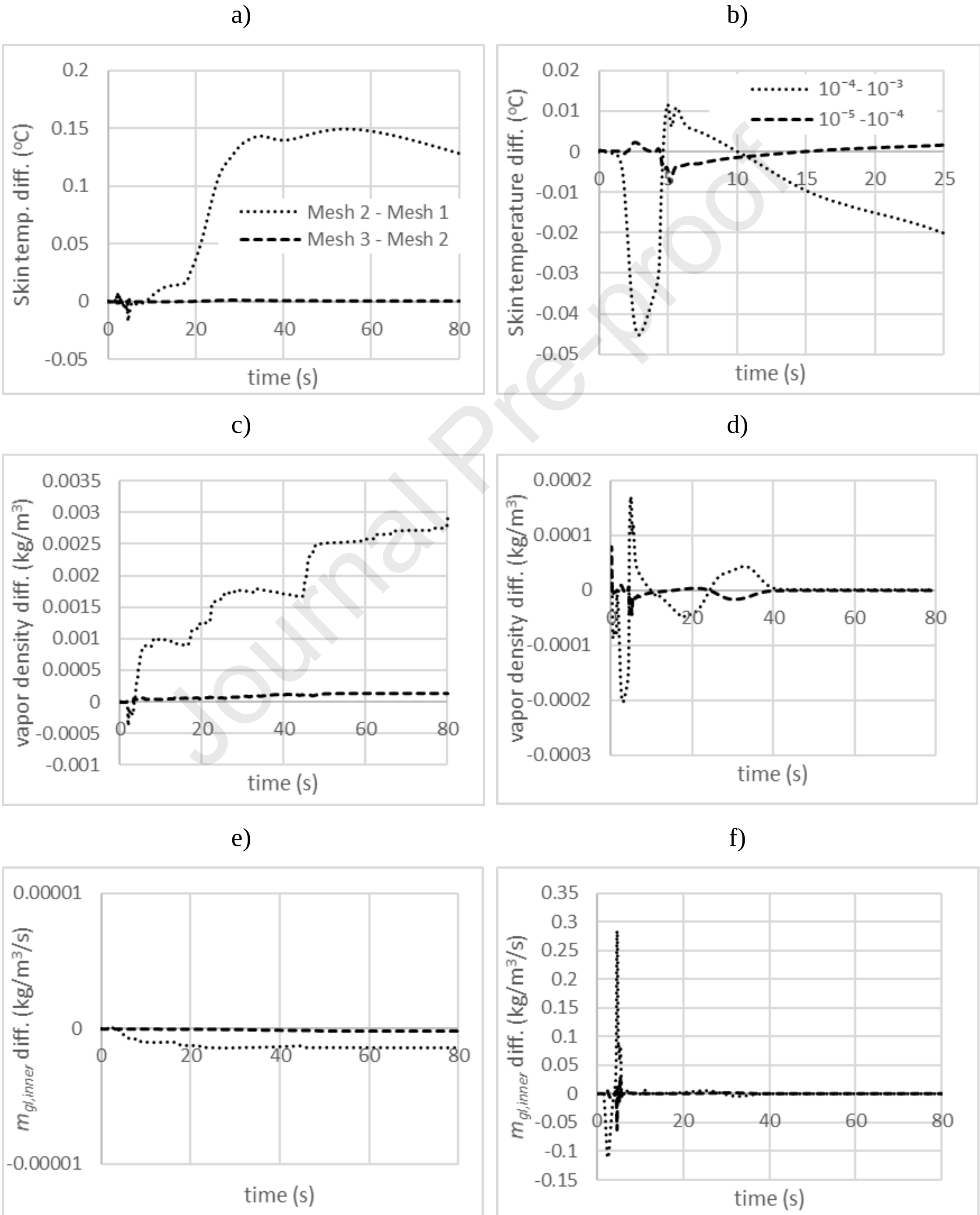

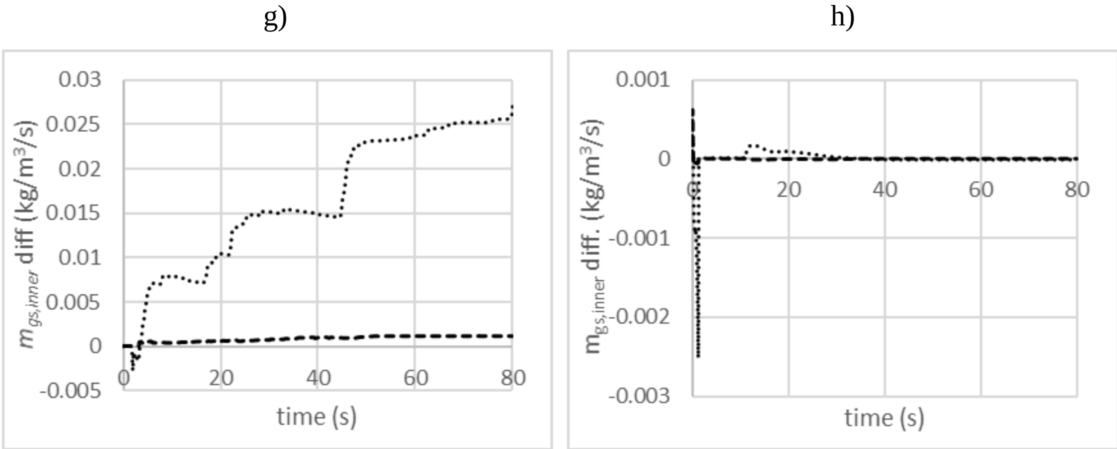

Figure 2 - Differences in the: a) skin temperature; c) water vapor densities; e) vaporization/condensation rate and; g)sorption rate histories near the skin, obtained with the indicated meshes. Differences in the: b) skin temperature d); water vapor densities; f) vaporization/condensation rate and; h) sorption rate histories near the skin, obtained with the indicated relative tolerances.

2.5 Model validation

The textile model was validated with the experimental results outlined in [6]. The firefighting jacket used in the experiments consists of an outer shell (93 % meta-aramid/5 % para-aramid/2 % antistatic), moisture barrier (P.T.F.E./nonwoven meta-aramid), and thermal inner (100 % para-aramid).

Before a heat exposure, the outer shell or/and thermal inner were initially pre-wetted. Then, a total heat flux of 15.4 kW/m^2 was irradiated on the outer shell through a quartz tube heat source. A skin simulant sensor was used to register the heat flux reaching the backside of the fabric. Such a sensor imitates the thermal properties of the skin. Thus its registered heat flux is then used as an input to calculate second–degree burn times using equations 8a-c and utilizing the properties outlined in Table 2 [6,24].

Figure 3 shows the obtained experimental and numerical skin temperatures and heat fluxes at the skin simulant sensor in the case where the outer shell fabric was initially saturated with water. Saturation corresponds to a wetness level of unity according to the wetting protocol utilized in [6].

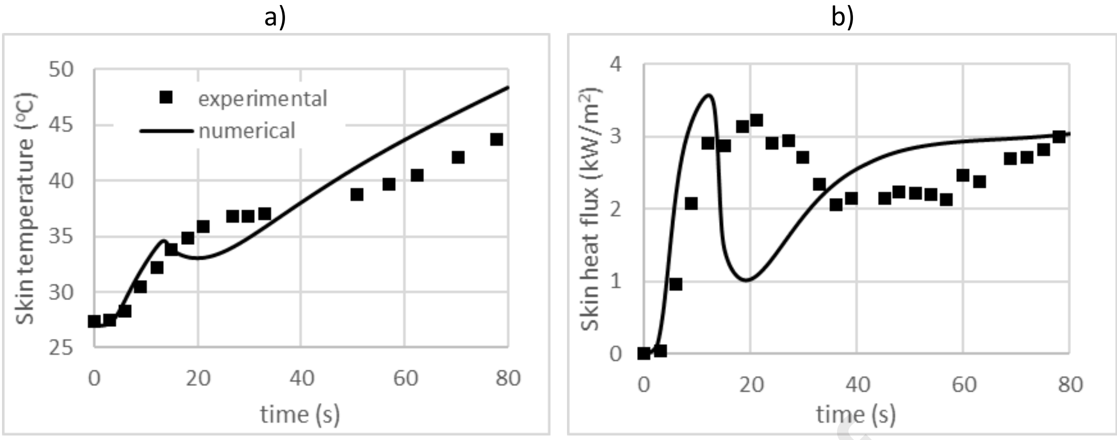

Figure 3 - Comparison between experimental [6] and numerical results for radiant exposure of 15.4 kW/m^2 for an outer shell initially saturated with water; a) skin temperature and b) skin heat flux over time

As can be seen, good agreement between numerical and experimental data is obtained. Initially, the firefighting garment is exposed to a heat hazard, which causes the moisture present in the outer shell to evaporate, forming steam. This steam is rejected towards the environment or diffuses throughout the textile layers, eventually reaching the skin. As the skin is at a much lower temperature than the heated steam, the vapor is sorbed in the fiber of the textile, close to the skin (i.e., thermal inner), and it also condenses, liberating latent heat and thus raising the skin temperature (i.e., Figure 3a and b, $5 < t < 15$ s). Once the moisture in the outer shell has fully evaporated, there is no more steam diffusing towards and condensing near the skin. The water present near the skin starts to evaporate as the temperatures in the textile are high due to the condensation which happened previously near the skin (i.e., evaporative cooling). This creates a sudden temperature fall (Figure 3a, $15 < t < 20$ s). In this phase, deviations from the experimental data in skin temperatures and skin heat fluxes are observed. Several reasons could be behind this deviation. The condensate could have dripped off the garment or wicked into the suit's outer layers, which are not considered in the numerical model. For $t > 20$ s, the skin temperature steadily rises due to the temperature increase in the fire protective clothing. At the same time, the evaporation of the condensate restrained in the thermal inner layer also takes place.

3. Results

3.1. Water presence in the outer shell

Figure 4a shows the second–degree burn times for the various exposure intensities and outer shell wetness levels considered. An increase in second-degree burn time with outer shell wetness level can be observed for all heat exposures considered. For example, for a heat exposure of 5 kW/m^2, a rise in the outer shell wetness level from 0 to 1 causes an increase in second-degree burn time from 71.7 s to 116.5 s. Such represents an increase of 62 % relative to the dry case (Figure 4b). However, the increase in second-degree burn time tends to be minor for higher heat fluxes. For example, considering exposure of 80 kW/m^2, the second-degree burn time rises from 17.8 s to 19.3 s when the outer shell wetness level increases from 0 to 1. According to Figure 4b, such represents a relative increase of 8 % compared to the dry case.

This minor increase in the protective effect for high heat fluxes is primarily due to the heat liberated by vapor condensation near the skin. Figure 5a shows the second-degree burn time when such heat is neglected in the simulations. As shown and expected, second-degree burn times are significantly greater, demonstrating how latent heat impacts thermal performance. For example, for a heat exposure of 5 kW/m^2, considering an initially saturated outer shell, the time to second-degree burn increases from 116.5 s to 136 s (Figure 4a and Figure 5a). Figure 5b illustrates the relative increase in second–degree burn time to show this effect clearly. As can be seen, there is a more significant increase in thermal performance with an increase in wetness level when compared to the original case (i.e., Figure 4b) for all heat exposures. For example, considering exposure of 80 kW/m^2, a relative increase in second-degree burn time of 37 % is achieved when steam condensation and sorption in the garment are not considered (Figure 5b). Instead, only an 8 % increase for a fully saturated outer shell is observed (Figure 4b).

In resume, for high-intensity exposures, both the steam condensation and sorption are responsible for at least a 29 % decrease in T.P.C. thermal performance. Such steam condensation tends to happen in the layers closest to the skin. Figure 4c shows the fraction of liquid water contained in the inner layer at the time of the second-degree burn (i.e., $f_{inner,\ 2nd}$). As can be seen, there is a decrease in the fraction of remaining liquid water with an increase in initial wetness level for all heat exposures considered. This behavior happens because a higher amount of water is initially present, (i.e. higher outer shell wetness level). And, as the amount of water condensing near the skin before a second-degree burn is more or less the same, its percentage representation decreases. Also, note that for heat fluxes above 20 kW/m^2, the remaining liquid water fraction tends to be independent of the heat flux exposure considered. This behavior happens because steam sorption and condensation in the thermal inner become major determinants to skin temperature rise and damage. Hence, when the presence of water in the outer shell is significant, the T.P.C could be designed in such a way as to mitigate the diffusion and condensation of water in the inner layers of the garment. In this way, significant gains in thermal performance can be achieved.

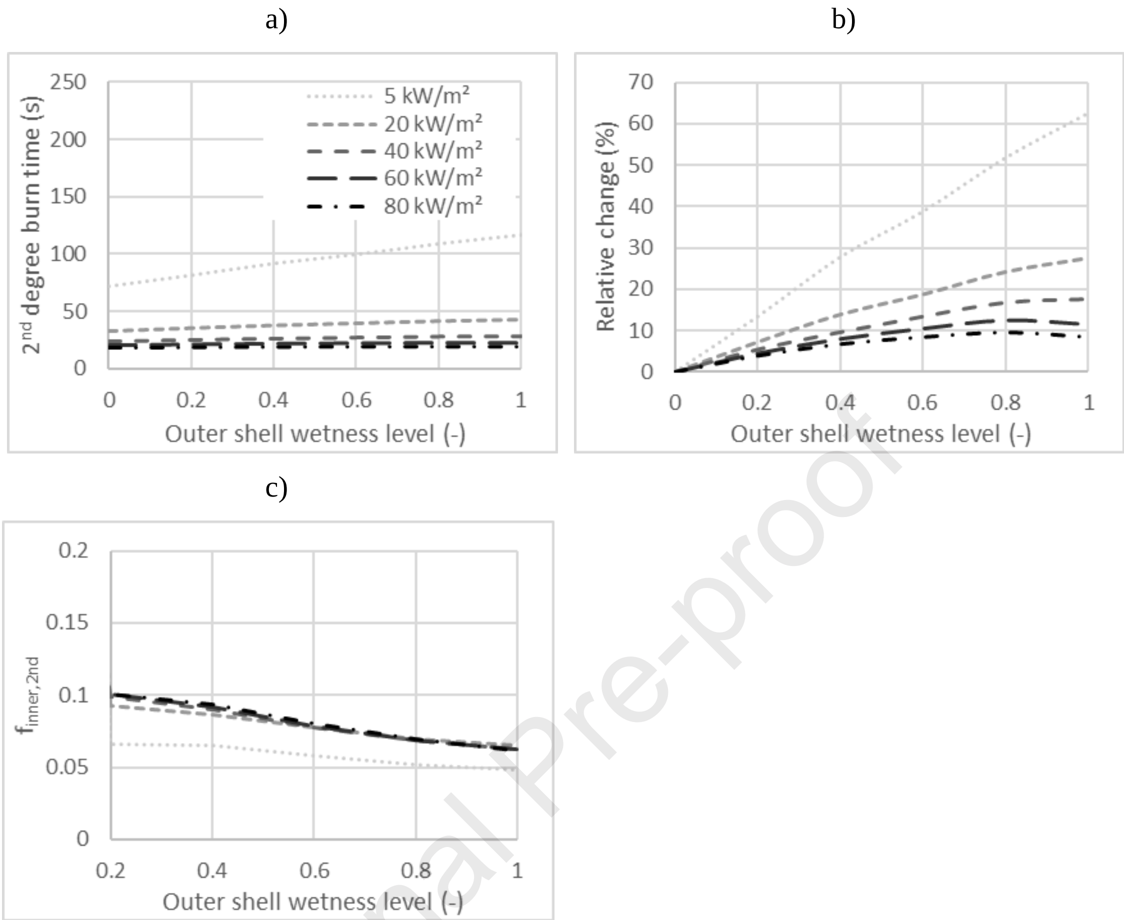

Figure 4 - a) second-degree burn times obtained for the indicated outer shell wetness levels and heat flux exposure intensities; b) relative change in second-degree burn time when compared to the dry case for corresponding wetness levels and heat fluxes; c) Remaining free water fraction ($f_{inner,2nd}$) in the thermal inner at the time when a second-degree burn occurs.

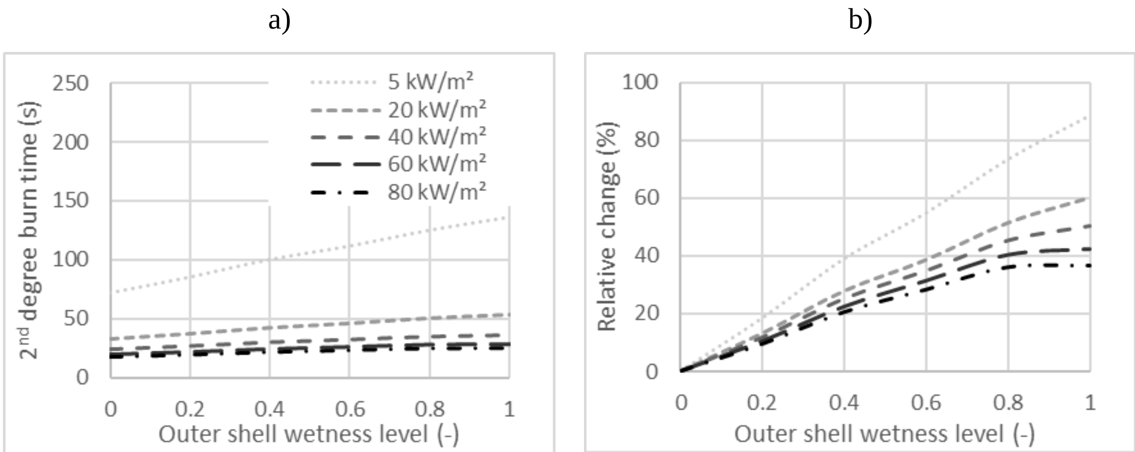

Figure 5 - Results obtained when condensation and sorption heat in the textile fiber are neglected: a) second-degree burn times for indicated heat fluxes and wetness levels in the outer shell; b) relative changes in second-degree burn times when compared to the dry case for the indicated outer shell wetness levels and heat exposures.

When a firefighter faces a low heat flux exposure, water in the outer shell increases second-degree burn time. However, the increase in thermal performance is marginal for higher heat fluxes due to more significant steam condensation near the skin. Hence, T.P.C. thermal performance can be considered independent of the water content in the outer shell for high heat fluxes. Steam burns may become common in such conditions. If this steam is prevented from reaching the skin by, for example, using less porous textiles [25], a significant rise in thermal performance can be achieved.

3.2. Water presence in the thermal inner

Figure 6a shows the second-degree burn times obtained for the indicated heat flux scenarios when the inner layer has different initial water content. For low heat flux exposures (i.e., 5 kW/m^2), second-degree burn time increases non - linearly with initial wetness level increase. This behavior is clearly observed when relative changes in second-degree burn times are considered (Figure 6b). There is a sharp linear increase in second-degree burn time for low heat fluxes (i.e., < 5 kW/m^2) for low initial water content. The linear increase is due to the onset of the latent heat associated with water desorption and vaporization. Then, the second-degree burn time decreases between wetness levels of 0.2 and 0.4, reaching a minimum, and steadily rises again (Figure 6b). This increase is justified because, when a large amount of water is present in the thermal inner, some of it will not evaporate, remaining in the clothing even after the firefighter obtains a second-degree burn (e.g., for a wetness level of 1, the inner layer contains around 60 % of the initial water content; Figure 6c). At the same time, water evaporation happens further away from the skin, and less vapor diffuses and condenses at the skin. This phenomenon occurs because the pores become more saturated as the initial presence of water increases.

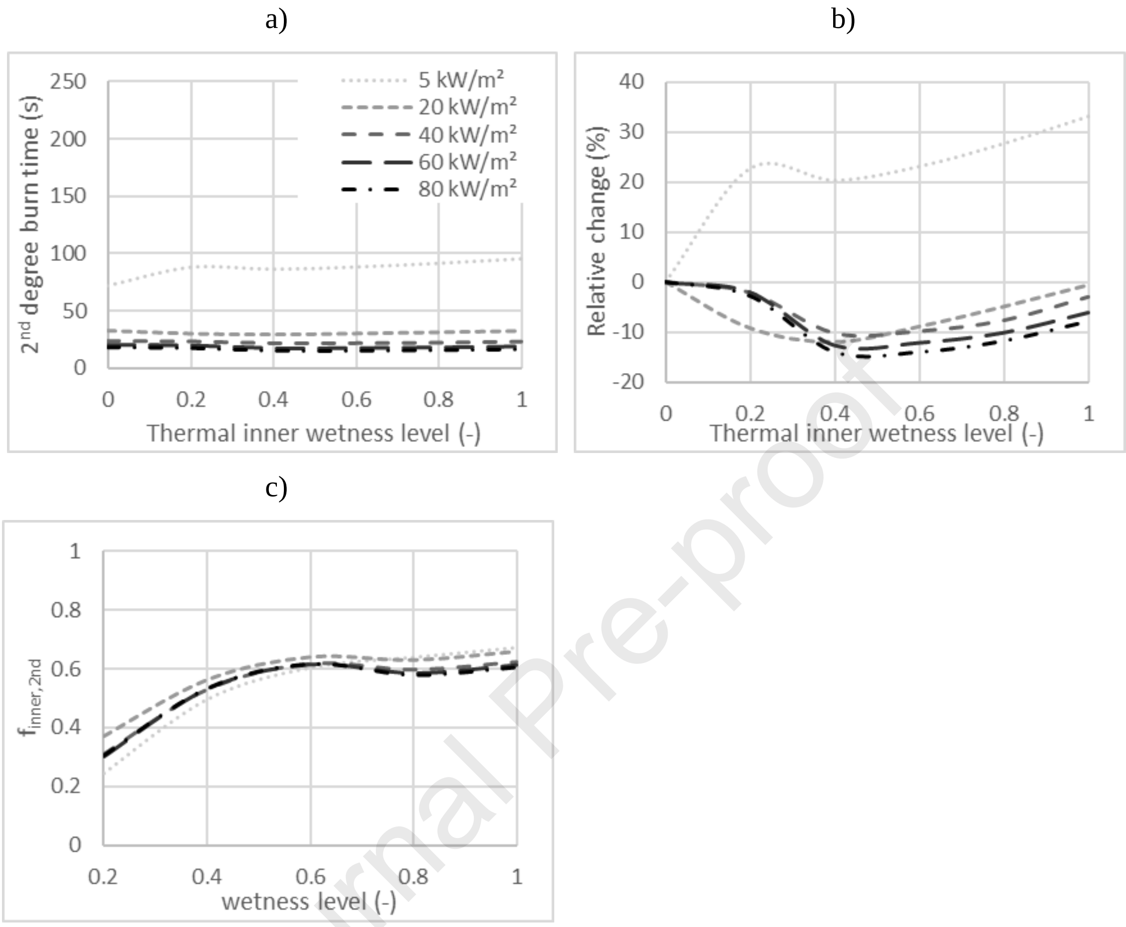

Figure 6 - a) second-degree burn times obtained for the indicated thermal inner wetness levels and heat flux exposure intensities; b) relative change in second degree burn time when compared to the dry case for corresponding wetness levels and heat fluxes; c) Remaining free water fraction ($f_{inner,2nd}$) in the thermal inner at the time when a second-degree burn occurs.

Second-degree burn time presents similar relationships for more significant heat fluxes, reaching a minimum at about 0.4 wetness level for heat exposures in the range of 20 to 80 kW/m^2 (Figure 6b).

However, above a certain wetness level, the second-degree burn time decreases relative to the dry case (e.g., Figure 6b, 20 kW/m^2, wetness level > 0.2). The quantity of steam that reaches the skin and condenses is significant enough to cause more heat transfer towards it. For greater wetness levels (above 0.5), similar to low heat fluxes, water is still present in the thermal inner after a second-degree burn time (Figure 6c). Phenomena associated with water vaporization and moisture condensation are behind the observed second-degree burn time tendencies.

To emphasize and show more clearly the steam phenomena discussed above, the relative and second-degree burn times without condensation phenomena should again be analyzed (Figure 7). The impact of moisture condensation on thermal performance is quite significant. For example, for an exposure of 20 kW/m^2 and initially saturated thermal inner, moisture sorption and condensation are responsible for a 225 % decrease in the thermal performance.

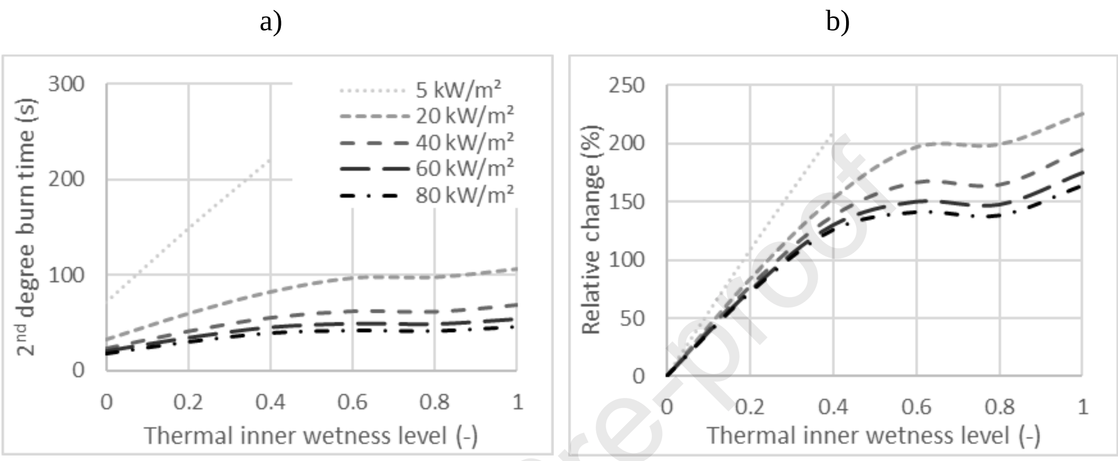

Figure 7 - Results obtained when condensation and sorption heat in the textile fiber are neglected: a) second-degree burn times for indicated heat fluxes and wetness levels; b) relative changes in second-degree burn times compared to the dry case for the indicated outer shell wetness levels and heat exposures.

Lastly, the liquid fraction present after the exposure in the thermal inner is quite significant, tending to a plateau of 0.6 with increasing wetness levels (Figure 6c). This behavior happens because steam sorption and condensation in the thermal inner become determinants for skin temperature rise and damage.

In conclusion, water presence in the thermal inner during firefighting can be prejudicial towards the firefighter for high heat fluxes. Solutions to mitigate such hazards and enhance thermal performance would have to ensure that the generated steam would be expelled to the environment rather than allowed to reach the firefighters' skin. An alternative would be, for example, to introduce a thermal inner with higher evaporative resistance but also a lower fiber fraction to not allow for moisture accumulation, decreasing steam burn risk.

3.3. Water presence in the outer shell and thermal inner

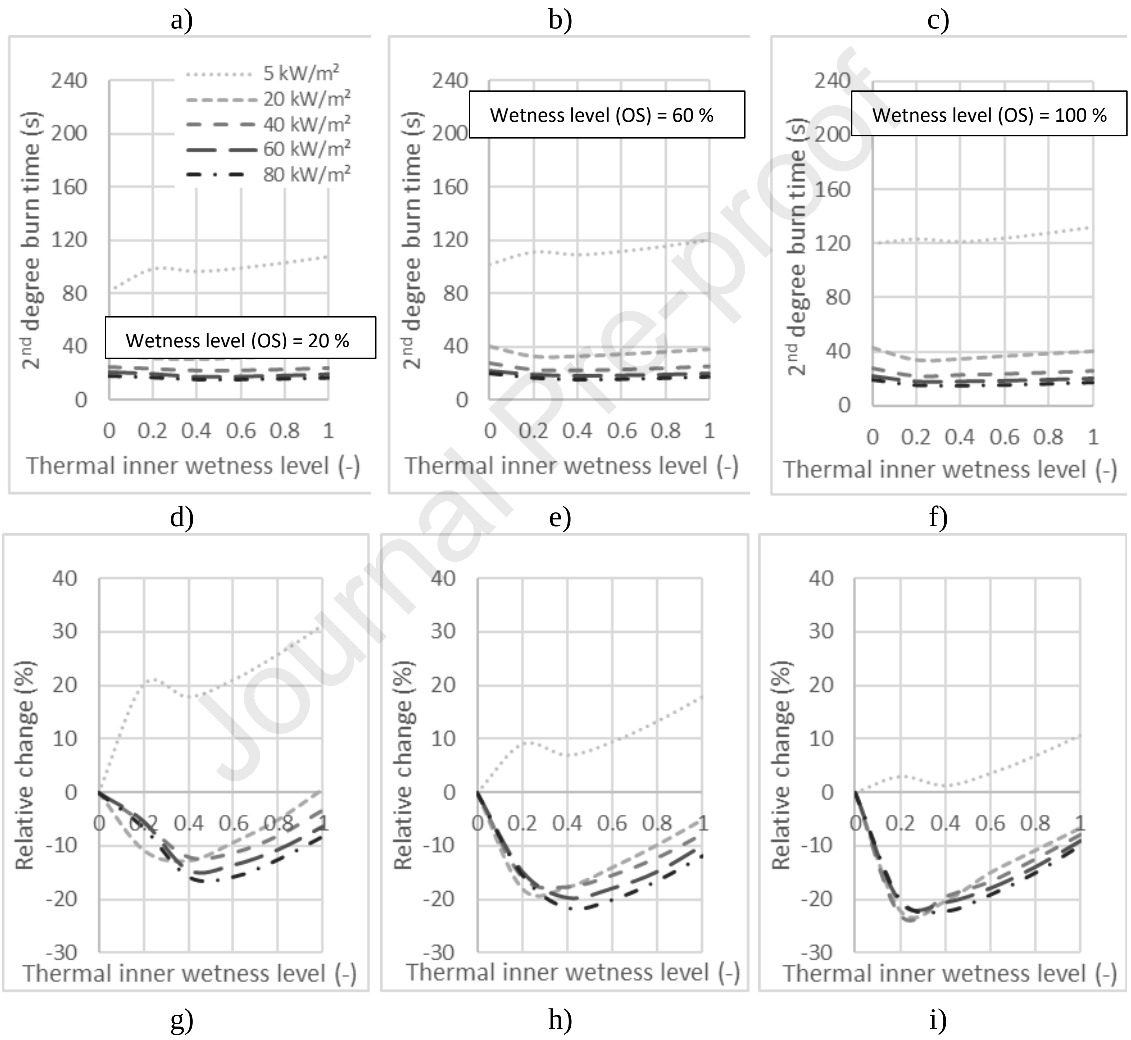
a)
b)
c)
240
200
160
120
80
40
0
2nd degree burn time (s)
5 kW/m²
20 kW/m²
40 kW/m²
60 kW/m²
80 kW/m²
Wetness level (OS) = 20 %
Wetness level (OS) = 60 %
Wetness level (OS) = 100 %
0 0.2 0.4 0.6 0.8 1
Thermal inner wetness level (-)
d)
e)
f)
40
30
20
10
0
-10
-20
-30
Relative change (%)
Thermal inner wetness level (-)
g)
h)
i)

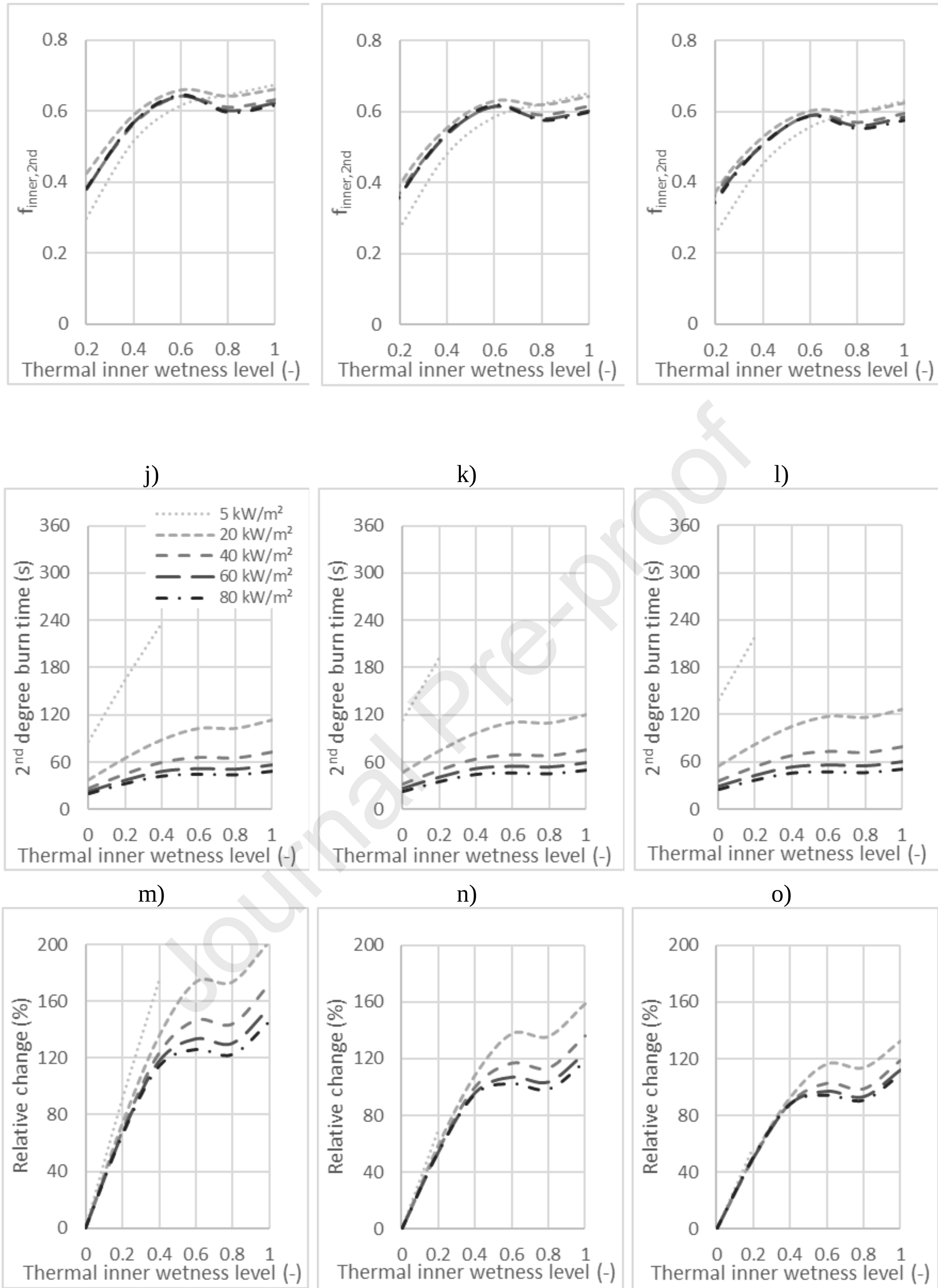

Figure 8 - a-c) Second-degree burn times obtained for the indicated outer shell (0.2, 0.6, and 1 wetness levels for a-c respectively) and thermal inner wetness levels, for different heat flux exposure intensities; d-f) relative change in second-degree burn time when compared to the dry case for corresponding wetness levels and heat fluxes; g-I) remaining free water fraction ($f_{inner,2nd}$) in the thermal inner when a second-degree burn occurs; j-l) second-degree burn times when no heat of condensation and sorption are considered in the textile; m-o) relative change in second-degree burn times when no heat of condensation and sorption are considered.

During a firefighter scenario, there may be situations where both the thermal inner and outer shell may be wet due to internal (e.g., sweating) and external (e.g., hose spraying) water sources. Hence in such cases, it is also of interest to study the thermal behavior of the T.P.C. Figure 8a-c shows the second-degree burn times for the indicated thermal inner wetness levels and wetness levels of 0.2, 0.6, and 1 in the outer shell, respectively. As can be seen for a heat flux exposure of 5 kW/m^2, the second-degree burn time rises with increased thermal inner and outer shell wetness levels. However, for heat flux exposures above 20 kW/m^2, the second-degree burn time tends to present a minimum trend for all outer shell wetness levels considered (Figure 8a-c). For example, for a wetness level of 0.2 in the outer shell and heat exposure of 20 kW/m^2, second-degree burn time shows a decreasing trend for thermal inner wetness levels between 0.2 - 0.4 (Figure 8a), reaching a minimum at 0.4 of about 30.9 s. It then rises for wetness levels above 0.4, reaching 35.6 s when saturated.

Relative second-degree burn times emphasize the variations that occur with thermal inner wetness levels (Figure 8d-f). For example, for a heat flux exposure of 5 kW/m^2, the relative rises in second-degree burn time barely pass the 30 % mark, independently of the outer shell initial wetness level. For higher heat fluxes, above 20 kW/m^2, the minimum trend with thermal inner wetness level is verified. For example, for an outer shell wetness level of 0.2, the minimum tends to happen around a thermal inner wetness level of 0.5, between -10 % and -20 % depending on the heat flux exposure considered (Figure 8d).

Steam condensation/sorption is mainly responsible for the second-degree burn tendencies with wetness levels obtained. Figure 8g-i show the remaining water liquid fraction at the thermal inner when the exposure ends for the various wetness levels. As can be seen, the remaining liquid fractions have similar values and tendencies to those obtained when only the thermal inner is initially wet (Section 3.3). This behavior was e expected as most of the water present in the outer shell evaporated and diffused towards the environment instead of the skin (Section 3.2). Figure 8j-l show the second-degree burn times when condensation/sorption phenomena are not taken into account. Compared to the original case (i.e., Figure 8a-c), we can observe that condensation heat near the skin plays a crucial role in decreasing thermal performance. For example, suppose the firefighter faces an exposure of 20 kW/m^2 when the wetness level at the outer shell is 0.6 and 0.2 at the thermal inner. In that case, the presence of steam condensation reaching the skin will account for a 41.7 s decrease in the second-degree burn time (Figure 8b and k). This effect represents a difference of 78 % in thermal performance.

In conclusion, when the water is present both in the outer shell and thermal inner, there tends to be an increase in thermal performance for low heat fluxes, while for high heat fluxes, a diminishing in thermal performance happens. However and once more, if correctly managed, the water present in the garment can positively impact thermal performance if it is not allowed to reach and condense near the skin.

3.4. Real heat flux scenario

The data and phenomena discussed in previous sections with constant heat fluxes can be applied to analyze the impact of moisture presence on thermal performance for firefighting exercises. Firefighters usually face non – constant heat exposures from the environment, and hence a real case heat flux from a live-fire training exercise will be considered in this section. The live training exercise was performed in a structure where firefighters wore heat flux sensors to monitor their heat exposure throughout the activity [26]. Below, the registered heat flux for the firefighting exercise is shown (Figure 9a).

a) b)

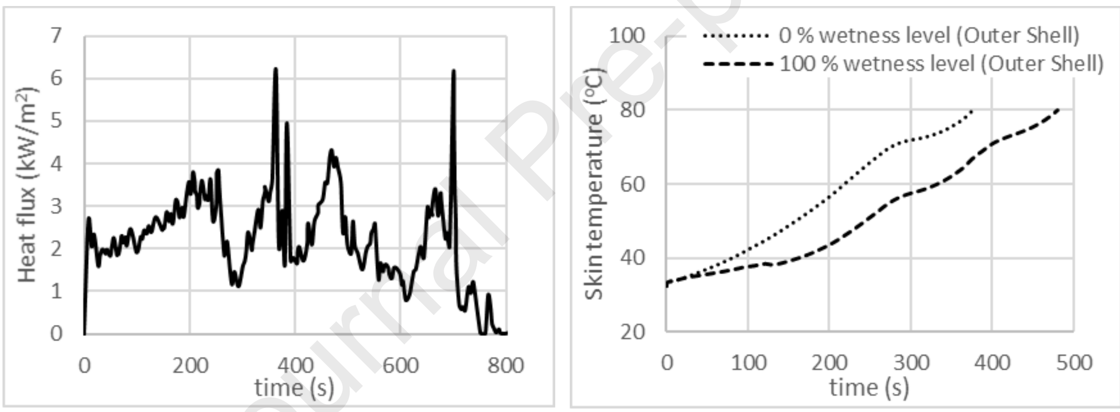

Figure 9 - a) heat flux data retrieved from a live-fire training exercise [26]; b) skin temperature obtained by simulation when the heat flux is considered a boundary condition for the indicated wetness levels.

Figure 9b shows the skin temperature profiles obtained when the textile is dry and when the outer shell is saturated. As can be seen, the temperature increase rate tends to vary over time, essentially due to the varying intensity of the external heat flux.

Figure 10a shows the second-degree burn time obtained for various inner and outer layer wetness levels. As is shown, an increase in second-degree burn time happens with an increase in thermal inner wetness level. This effect was expectable because the radiated heat flux is low–intensity (Figure 10a). Also, the increase in outer shell wetness level causes an increase in second-degree burn time. Relative increases in second-degree burn time are also more significant when the outer shell is dry (about 50 % increase when the inner layer is fully saturated; Figure 10b). Figure 10c shows the fractions of free water obtained after the exposure. And as can be seen, the tendencies are similar to those obtained when constant heat fluxes were simulated in the previous sections for low heat fluxes.

Hence, the data and phenomena discussed in previous sections with constant heat fluxes can explain the tendencies observed in thermal behavior and guide possible thermal performance improvement solutions.

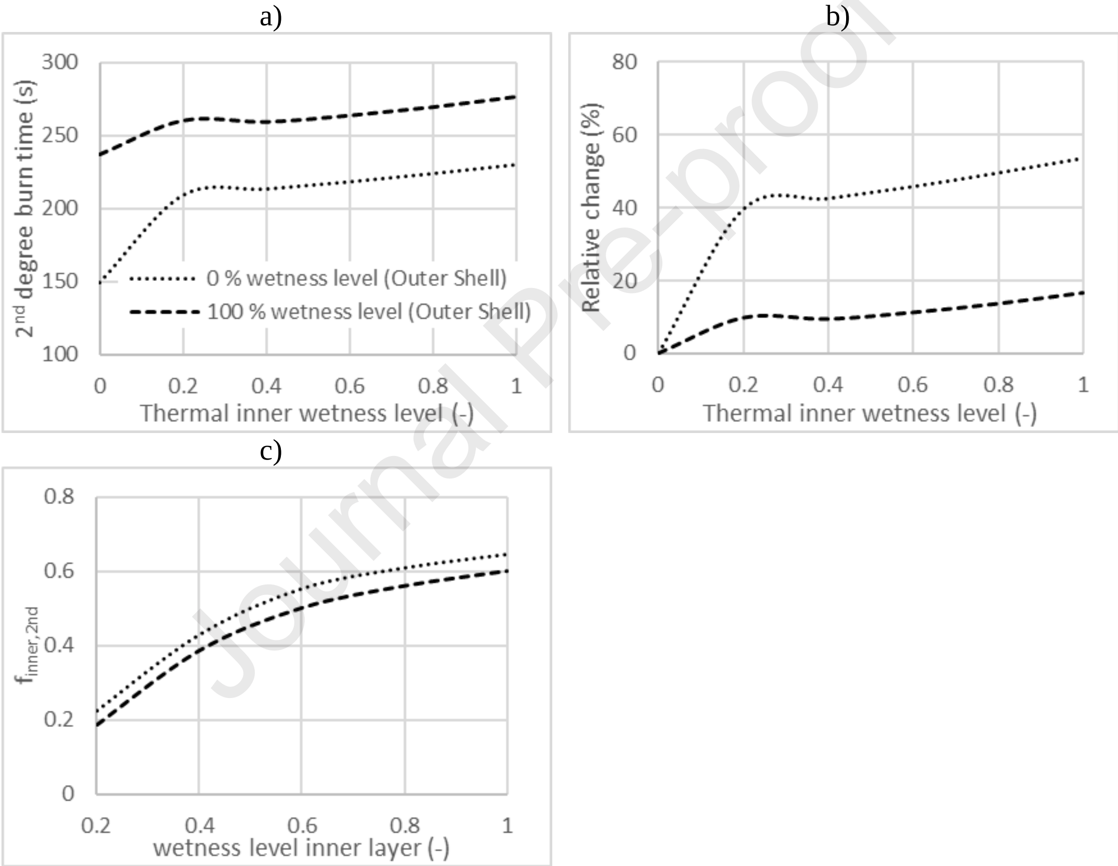

Figure 10 - a) second degree burn times obtained for the indicated outer shell and thermal inner wetness levels; b) relative change in second-degree burn time when compared to the dry case for corresponding wetness levels; c) remaining free water fraction ($f_{inner,2nd}$) in the thermal inner at the time when a second-degree burn occurs.

4. Conclusions

In this study, a one-dimensional numerical analysis of heat and moisture transport in a 3 –layered firefighting garment was performed. The thermal performance according to a second-degree burn criterion was analyzed. Different initial moisture quantities present in the inner layer and outer shell and different heat flux exposures were considered to generate maps and identify conditions for which moisture presence was impactful, specifying the reasons. The following specific conclusions were obtained:

- The presence of moisture in the outer shell increases second–degree burn time. However, this increase tends to be marginal for high heat fluxes (above 20 kW/m^2). Hence, moisture in the outer shell does not influence thermal performance for high heat fluxes.
- The presence of moisture in the inner layer generally decreases second-degree burn time and shows the worse performance at a wetness level of 50 % for heat flux exposures above 20 kW/m^2. For low-intensity exposure, however, the presence of moisture increases second-degree burn time.
- The simultaneous presence of water in the outer shell and thermal inner causes an increase in second-degree burn time, but only for low heat exposures (i.e., 5 kW/m^2). For higher heat exposures, it decreases and shows a minimum trend with the thermal inner wetness level.
- Decreases in thermal performance, especially for high heat fluxes, are essentially due to moisture condensation near the skin, as the liberated heat will provoke scald burns.

Lastly, it is essential to note that if we prevent the water vapor from reaching the skin, water in the textile, in all cases, provides significant gains in second-degree burn time. Nevertheless, in practical terms, such is challenging to achieve as the firefighter sweats and water vapour must be allowed to be released from the skin to the environment; otherwise, the firefighter might overheat.

However, a good textile selection contributes to noteworthy gains in thermal performance. One of the options that is currently gaining attention in the literature is to use janus wetting and wicking properties to allow for better moisture management [27]. The authors would also like to point out that in a future study, textile compression phenomena could be incorporated in the model, as in such, situations burn injuries could occur due to the movement of hot water in the textile assembly and not necessarily due to steam condensation near the skin [28].

5. Appendix

5.1 Influence of an air gap

Figure 11 shows the second–degree burn times obtained when there is no air gap and when a 6.4 mm air gap is considered. The model described in section 2.2. was slightly modified to include the air gap domain (between fabric and skin) and conductive and radiative heat transport (assuming both skin and fabric to be grey bodies with an emissivity of 0.9) through it. Water vapor transport was considered to occur through the air gap where condensation could occur according to an equation similar to eq. 5b. Instantaneous condensation could happen in the air gap due to the presence of a nuclei in the air (e.g., dust particles).

The addition of an air gap between the fabric and the skin will cause a positive shift in the second-degree burn – times obtained for the various wetness levels. Such shifts roughly represent increases of about a factor of 2 when an air gap of 6.4 mm is present. In this work, the authors intended to simulate the worst possible case scenario where vapour mass transfer and heat transfer towards the skin would be the greatest. And such happens when no air gaps are considered. The addition of an air gap does not change the quality of the results generated (Figure 11). Except for the resistance role of the air gap, no new physical phenomena are observed when an air gap is considered.

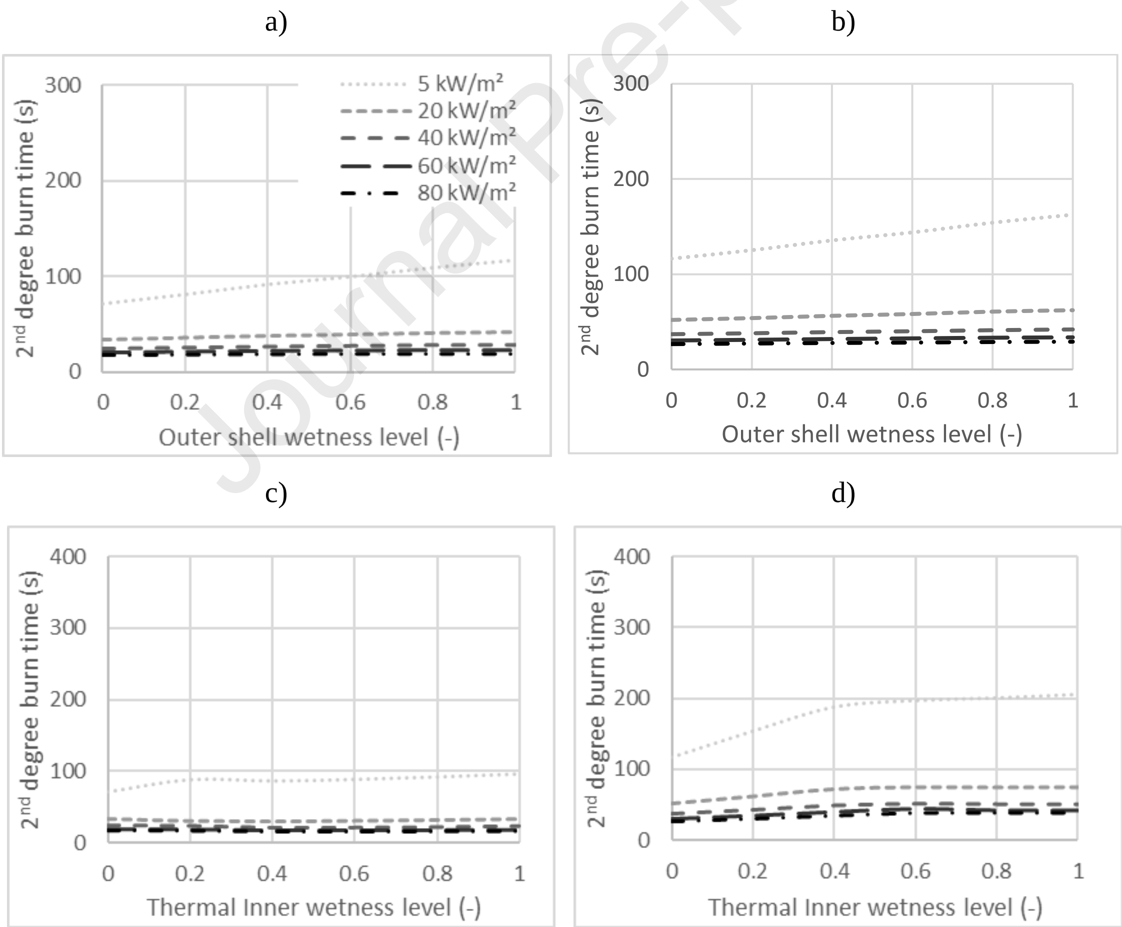

Figure 11 - Second degree - burn times obtained for indicated wetness levels considering: a,c.) no air gap b,d.) 6.4 mm air gap between skin and fabric.

6. Acknowledgments

National funds supported the present study through F.C.T. –Fundação para a Ciência e a Tecnologia, I.P., within the scope of the project UIDB/00532/2020 as well as by PCIF/SSO/0106/2018 - Project for "Development of an innovative firefighter's jacket", funded by national funds through FCT/MCTES (PIDDAC). Malaquias acknowledges the financial support provided by F.C.T. through the PhD Grant PD/BD/ 135097/2017.

7. References

[1] A. Morel, G. Bedek, F. Salaün, D. Dupont, A review of heat transfer phenomena and the impact of moisture on firefighters’ clothing and protection, Ergonomics. 57 (2014) 1078–1089. https://doi.org/10.1080/00140139.2014.907447.

[2] A.M. Raimundo, A.R. Figueiredo, Personal protective clothing and safety of firefighters near a high intensity fire front, Fire Saf. J. 44 (2009) 514–521. https://doi.org/10.1016/j.firesaf.2008.10.007.

[3] J.R. Prasad, K., Twilley, W. H., & Lawson, Thermal Performance of Fire Fighters’ Protective Clothing: Numerical Study of Transient Heat and Water Vapor Transfer., Natl. Inst. Stand. Technol. Gaithersburg, MD 20899-8660. (2002) 1–32.

[4] C. Keiser, P. Wyss, R.M. Rossi, Analysis of steam formation and migration in firefighters’ protective clothing using x-ray radiography, Int. J. Occup. Saf. Ergon. 16 (2010) 217–229. https://doi.org/10.1080/10803548.2010.11076839.

[5] Y. Su, J. Li, G. Song, The effect of moisture content within multilayer protective clothing on protection from radiation and steam, Int. J. Occup. Saf. Ergon. 24 (2018) 190–199. https://doi.org/10.1080/10803548.2017.1321890.

[6] H. Zhang, G. Song, H. Ren, J. Cao, The effects of moisture on the thermal protective performance of firefighter protective clothing under medium intensity radiant exposure, Text. Res. J. 88 (2018) 847–862. https://doi.org/10.1177/0040517517690620.

[7] L.K. Lawson, E.M. Crown, M.Y. Ackerman, J.D. Dale, Moisture effects in heat transfer through clothing systems for wildland firefighters, Int. J. Occup. Saf. Ergon. 10 (2004) 227–238. https://doi.org/10.1080/10803548.2004.11076610.

[8] M. Guan, A. Psikuta, M. Camenzind, J. Li, S. Mandal, R. Michel Rossi, S. Annaheim,

Effect of perspired moisture and material properties on evaporative cooling and thermal protection of the clothed human body exposed to radiant heat, Text. Res. J. 89 (2019) 3663–3676. https://doi.org/10.1177/0040517518817067.

[9] H. He, Z.C. Yu, G. Song, The effect of moisture and air gap on the thermal protective performance of fabric assemblies used by wildland firefighters, J. Text. Inst. 107 (2016) 1030–1036. https://doi.org/10.1080/00405000.2015.1083258.

[10] R.L. Barker, C. Guerth-Schacher, R. V. Grimes, H. Hamouda, Effects of Moisture on the Thermal Protective Performance of Firefighter Protective Clothing in Low-level Radiant Heat Exposures, Text. Res. J. 76 (2006) 27–31. https://doi.org/10.1177/0040517506053947.

[11] C. Keiser, R.M. Rossi, Temperature Analysis for the Prediction of Steam Formation and Transfer in Multilayer Thermal Protective Clothing at Low Level Thermal Radiation, Text. Res. J. 78 (2008) 1025–1035. https://doi.org/10.1177/0040517508090484.

[12] E. Onofrei, T.C. Codau, S. Petrusic, G. Bedek, D. Dupont, D. Soulat, Analysis of moisture evaporation from underwear designed for fire-fighters, Autex Res. J. 15 (2015) 35–47. https://doi.org/10.2478/aut-2014-0015.

[13] P. Chitrphiromsri, Modeling of Thermal Performance of Firefighter Protective Clothing during the Intense Heat Exposure, NCSW, 2004.

[14] Y. Su, J. Li, X. Zhang, A Coupled Model for Heat and Moisture Transport Simulation in Porous Materials Exposed to Thermal Radiation, Transp. Porous Media. 131 (2020) 381–397. https://doi.org/10.1007/s11242-019-01347-2.

[15] D. Huang, S. He, Influence of Initial Moisture Content on Heat and Moisture Transfer in Firefighters' Protective Clothing, Sci. World J. 2017 (2017). https://doi.org/10.1155/2017/9365814.

[16] P. Łapka, P. Furmański, Modeling and analysis of the influence of the protective garment movement on the skin temperature and burn degree, Fire Saf. J. 111 (2020). https://doi.org/10.1016/j.firesaf.2019.102916.

[17] DuPont, Technical Guide for NOMEX Brand Fiber, 2001.

[18] J.W.S. Hearle, M.W. E, Physical Properties of Textile Fibres, 4th ed., Woodhead Publishing Limited, 2008.

[19] S.F. Neves, J.B.L.M. Campos, T.S. Mayor, On the determination of parameters required for numerical studies of heat and mass transfer through textiles - Methodologies and

experimental procedures, Int. J. Heat Mass Transf. 81 (2015) 272–282. https://doi.org/10.1016/j.ijheatmasstransfer.2014.09.038.

[20] D.A. Torvi, Heat transfer in thin fibrous materials under high heat flux conditions, 1997.

[21] P. Gibson, Governing Equations for Multiphase Heat and Mass Transfer in Hygroscopic Porous Media With Applications to Clothing Materials, 1994.

[22] F.C. Henriques, Studies of thermal injury V. The predictability and the significance of thermally induced rate processes leading to irreversible epidermal injury, Arch. Pathol. 43 (1947) 489–502.

[23] M.K. Donnelly, W.D. Davis, J. Lawson, M. Selepak, Thermal Environment for Electronic Equipment Used by First Responders, Natl. Inst. Stand. Technol. Spec. Publ. 1474. (2006) 41.

[24] H. Zhang, G. Song, Y. Gu, H. Ren, J. Cao, Effect of moisture content on thermal protective performance of fabric assemblies by a stored energy approach under flash exposure, Text. Res. J. 88 (2018) 1847–1861. https://doi.org/10.1177/0040517517712097.

[25] Y. Su, R. Li, G. Song, J. Li, C. Xiang, Modeling steam heat transfer in thermal protective clothing under hot steam exposure, Int. J. Heat Mass Transf. 120 (2018) 818–829. https://doi.org/10.1016/j.ijheatmasstransfer.2017.12.074.

[26] J.M. Willi, G.P. Horn, D. Madrzykowski, Characterizing a Firefighter's Immediate Thermal Environment in Live-Fire Training Scenarios, Fire Technol. 52 (2016) 1667–1696. https://doi.org/10.1007/s10694-015-0555-1.

[27] X. Guan, X. Wang, Y. Huang, L. Zhao, X. Sun, H. Owens, J.R. Lu, X. Liu, Smart Textiles with Janus Wetting and Wicking Properties Fabricated by Graphene Oxide Coatings, Adv. Mater. Interfaces. 8 (2021). https://doi.org/10.1002/admi.202001427.

[28] S. Mandal, G. Song, F. Gholamreza, A novel protocol to characterize the thermal protective performance of fabrics in hot-water exposure, J. Ind. Text. 46 (2016) 279–291. https://doi.org/10.1177/1528083715580522.

Conflicts of interest

The authors declare no conflicts of interest.

Sample CRediT author statement

Andre Fonseca Malaquias: Conceptualization, Methodology, Software, Validation, Formal analysis Investigation, Writing – Original Draft. **S.F.Neves:** Methodology, supervision, Writing – Review & Editing, Funding Acquisition **J.B.L.M Campos:** Supervision, Methodology, Writing – Review & Editing, Funding Acquisition